Research Article

Abdul Hamid Ganie, Humaira Yasmin*, Aisha A. Alderremy*, Azzh Saad Alshehry, and Shaban Aly

Fractional view analytical analysis of generalized regularized long wave equation

https://doi.org/10.1515/phys-2024-0025
received December 22, 2023; accepted April 15, 2024

Abstract: In this research study, we focus on the generalized regularized long wave equation and the modified regularized long wave equation, which play pivotal roles in characterizing plasma waves in oceans and ion acoustic waves in shallow water, a domain deeply rooted in physical phenomena. Employing two computational techniques, namely, the optimal auxiliary function method and the Laplace iterative transform method, we approximate these equations. These formulas are used to characterize plasma waves in oceans and ion acoustic waves in shallow water. The results discovered have important ramifications for our comprehension of many physical events. Our results show that both methods are robust, easy to use, and successful. Both methods yield results that are satisfactory to each other. With the use of tables and graphs, we compared the two suggested approaches. The findings suggest that the suggested methods can be widely applied to explore other real-world problems.

Keywords: optimal auxiliary function method, Laplace iterative transform method, generalized regularized long wave equation, modified regularized long wave equation

*** Corresponding author: Humaira Yasmin,** Department of Basic Sciences, General Administration of Preparatory Year, King Faisal University, P.O. Box 400, Al Ahsa, 31982, Saudi Arabia; Department of Mathematics and Statistics, College of Science, King Faisal University, P.O. Box 400, Al Ahsa, 31982, Saudi Arabia, e-mail: hhassain@kfu.edu.sa
*** Corresponding author: Aisha A. Alderremy,** Department of Mathematics, Faculty of Science, King Khalid University, Abha 61413, Saudi Arabia, e-mail: aaldramy@kku.edu.sa
Abdul Hamid Ganie: Basic Science Department, College of Science and Theoretical Studies, Saudi Electronic University, Riyadh 11673, Saudi Arabia, e-mail: a.ganie@seu.edu.sa
Azzh Saad Alshehry: Department of Mathematical Sciences, Faculty of Sciences, Princess Nourah Bint Abdulrahman University, P.O. Box 84428, Riyadh, 11671, Saudi Arabia, e-mail: asalshihry@pnu.edu.sa
Shaban Aly: Department of Mathematics, Faculty of Science, AL-Azhar University, Assiut, Egypt, e-mail: shaban.aly.201@azhar.edu.eg

1 Introduction

Fractional calculus is a field that is now seeing a lot of activity and is drawing the interest of many academics and professionals worldwide. The origins of this field can be found in a conversation between two well-known mathematicians that took place around 1695. There was not a sufficient response to the search for the definition of a function's half derivative. However, it is predicted that fractional calculus, which makes use of differentials and integrals of any order, will eventually eclipse traditional calculus, in which derivatives and integrals are restricted to integer orders [1–4]. Fractional-order mathematical models, however, have shown to be extremely useful in a variety of scientific and engineering fields [5–7]. As such, a great deal of attention has been paid to solving the issues that result from these areas. Numerous nonlinear processes have been modeled extensively using fractional-order differential and integral equations [8,9]. In the context of mathematical modeling of physical processes, fractional derivatives are more advantageous than integer order derivatives. It is common to see the application of fractional derivatives in systems biology research. Moreover, fractional derivatives are essential to the mathematical modeling of many different kinds of physical issues. In the realm of oceanic engineering, the use of mathematical modeling to the study of tidal oscillations and tsunamis offers one example [10–12]. These equations can also find use in engineering disciplines, including flatness analysis, prediction of harmonic interactions, refractive prediction and diffraction, and refractive prediction in the area of coastal constructions. Nonlinear evolutionary equations hold significant importance across diverse disciplines including solid-state physics, biology, chemical physics, oceanic engineering, astrophysics, fiber optics, and plasma physics. There are several strategies available for addressing the approximate solutions to FDEs in the context of physical problems, sometimes referred to as perturbation methods. These techniques exhibit a high degree of precision and effectiveness in solving nonlinear fractional differential equations [13–17]. The current investigation relates two cases of time-fractional nonlinear partial differential equations [18–23]:

$$\frac{\partial^{\varphi}\mathcal{W}}{\partial\Omega^{\varphi}} + \frac{\partial\mathcal{W}}{\partial\Psi} + \mathcal{W}\frac{\partial\mathcal{W}}{\partial\Psi} + \frac{\partial^{3}\mathcal{W}}{\partial\Psi^{2}\partial\Omega} = 0, \quad \Omega > 0, \Psi \in \mathbb{R}, 0 < \varphi \leq 1, \tag{1}$$

$$\frac{\partial^{\varphi}\mathcal{W}}{\partial\Omega^{\varphi}} + \frac{\partial\mathcal{W}}{\partial\Psi} + 6\mathcal{W}^{2}\frac{\partial\mathcal{W}}{\partial\Psi} - \xi\frac{\partial^{3}\mathcal{W}}{\partial\Psi^{2}\partial\Omega} = 0, \quad \Omega > 0, \Psi \in \mathbb{R}, 0 < \varphi \leq 1. \tag{2}$$

Eq. (1) is known as the time-fractional nonlinear generalized regularized long wave (GRLW) equation, while Eq. (2) is known as the time-fractional nonlinear modified regularized long wave (MRLW) equation. In Eqs. (1) and (2), the derivative is represented in the Caputo sense of order φ. $\mathcal{W}(\Psi, \Omega)$ shows the probability density function, Ω is the temporal, and Ψ is the spatial coordinate. ξ shows the positive parameter.

The regularized long wave (RLW) equations have application in many areas, including magneto-hydrodynamics waves in plasma, ion-acoustic waves in plasma, rotating flow down a tube, longitudinal dispersive waves in elastic rods, and pressure waves in liquid–gas bubble mixtures. The RLW equations are regarded as significant equations for various essential physical systems in the fields of applied physics and engineering. In addition, this simulation includes many fluid flow challenges, which involve significant considerations of either viscous dissipation or shock dissipation. Moreover, it has the potential to be utilized in the modeling of dissipation-related nonlinear wave propagation problems. The dissipation observed in this context can be attributed to several factors, such as heat conduction, mass diffusion, thermal radiation, viscosity, chemical reactions, or other sources, depending on the specific modeling of the situation [21–23]. The RLW equations were formulated by Peregrine as a mathematical framework for studying solitons and modeling small amplitude long waves occurring on the outer layer of water. The present model serves as an alternative to the Korteweg-de Vries (KdV) equation in the investigation of soliton solutions. Secondary solitary waves are generated from the collision of two solitary waves, which are alternatively referred to as sinusoidal solutions. The aforementioned attribute holds significant importance within the context of the RLW equation. This characteristic exhibits similarities to the phenomenon of particle collisions, which give rise to the production of additional particles and radiation in the field of subatomic physics. Hence, the examination of the RLW equations yields insights into the phenomenon of generating secondary solitary waves and radiations, which can be linked to mechanisms observed in the field of particle physics. The nature of collisions between solitary waves in the RLW equations differs from that of collisions between solitary waves in the KdV equation. The soliton of the KdV equation exhibits interactions, collisions, and subsequent emergence without interruption, except for a phase change. The soliton of the RLW equations demonstrates the phenomenon wherein two solitary waves can interact by passing through each other, resulting in a reduction in amplitude and the generation of secondary waves. In addition to this, it is possible for a notch to appear in the negative amplitude wave. The aforementioned notch undergoes a transformation and develops into a subsequent wave characterized by negative amplitude. The phenomenon of wave amplitude shifting in opposite ways can lead to the creation and elimination of many secondary waves with both positive and negative amplitudes. The presence of several secondary waves could potentially give rise to sinusoidal residual effects, which manifest as radiation. The numerical formulation for the RLW equations was presented by Benjamin in 1972. The RLW equations are reliant upon the principles of conservation, including the conservation of mass, momentum, energy, and others [24,25]. The fractional RLW equations are also utilized to clarify some significant phenomena within the domain of ocean engineering and science, including shallow water waves characterized by long wavelengths and small amplitudes. The FRLW equations, which describe nonlinear waves, have garnered significant attention from researchers studying shallow water waves in oceanic environments. The mathematical modeling of nonlinear waves in the ocean was carried out using the FRLW equations. In addition, the FRLW equations are utilized to explain the phenomenon of Tsunamis, which are characterized by the presence of massive ocean waves. The large-scale internal waves that occur within the ocean depths as a result of temperature variations, posing a potential threat to naval boats, can be effectively modeled using the FRLW equations in a novel manner. Benjamin *et al.* [25] introduced the adoption of the RLW equations as a more favorable option compared to the traditional KdV equations for the analysis and interpretation of a wide range of physical phenomena in the fields of ocean engineering and science. The study of solitary waves has received significant attention in the field of ocean wave research. When two or three solitary waves encounter, it has been observed that these waves tend to maintain their shape. However, certain investigations have indicated the presence of a little tail emerging after the collision occurs. However, these characteristics have prompted researchers to conduct extensive investigations in the realm of ocean waves during the past few decades, employing both computational and analytical techniques to solve the associated problems. The FRLW equations provide the capability to effectively characterize numerous maritime engineering problems encountered in the actual world, offering a simplified approach. The time-fractional nonlinear MRLW equation and the time-fractional

nonlinear GRLW equation have approximate solutions, which is the aim of the current work. We use two computational approaches to solve the stated problems: the iterative Laplace transform technique and the optimal auxiliary function method (OAFM). Hammad *et al.* [26] first presented the idea of OAFM as a way to get approximate analytical solutions for the motion of a fourth-grade fluid on a vertical cylinder. This methodology offers an effective strategy for managing the convergence of the approximation solutions through the utilization of convergence-control parameters. In the past few years, the examination of this particular process has garnered significant attention from numerous scholars, emerging as a tool of significant potential in various domains within the areas of natural sciences and engineering. The OAFM is utilized to address the nonlinear differential equation associated with the Blasius problem [27]. The approximate solution for the thin film flow of a third-grade fluid on a moving belt problem is obtained using optimal auxiliary functions [28]. The Laplace iterative transform method (LITM) was utilized in our study to evaluate the proposed models, which combines the Laplace transform with the novel iterative approach (NIM) introduced by Jafari *et al.* [29].

2 Preliminaries

In this context, we present a set of fundamental definitions related to fractional calculus.

Definition 2.1. The Riemann–Liouville fractional integral is mathematically defined as follows [30]:

$$J^{\varphi}\mathcal{W}(\Psi) = \frac{1}{\Gamma(\varphi)}\int_0^{\varphi}\frac{\mathcal{R}(\mathcal{U})}{(\varphi-\mathcal{U})^{1-\varphi}}\mathrm{d}\mathcal{U},\ \varphi>0,\ \varphi>0, \tag{3}$$

$$J^{\varphi}\mathcal{W}(\Psi) = \mathcal{W}(\Psi).$$

In the above equation, Γ represents the Gamma function.

Definition 2.2. In the Caputo sense, fractional derivative is given by [33],

$$\begin{aligned}\mathcal{D}^{\varphi}\mathcal{W}(\Omega) &= J^{k-\varphi}\mathcal{W}(\Omega)\mathcal{D}^{k}\mathcal{W}(\Omega)\\ &= \frac{1}{\Gamma(k-\varphi)}\int_0^{\Omega}(\Omega-\beta)^{k-\varphi-1}\mathcal{W}^{(k)}(\beta)\mathrm{d}\beta,\end{aligned} \tag{4}$$

where

$$k-1<\varphi\le k,\quad k\in N,\quad h>0.$$

Definition 2.3. For the function $\mathcal{W}(\Psi,\Omega)$ the Caputo time-fractional differential operator of order φ, where k is the smallest integer that exceeds φ, is defined as follows [31,32].

$$\begin{aligned}\mathcal{D}_{\Omega}^{\varphi}\mathcal{W}(\Psi,\Omega) &= \frac{\partial^{\varphi}\mathcal{W}(\Psi,\Omega)}{\partial\Omega^{\varphi}}\\ &= \frac{1}{\Gamma(k-\varphi)}\int_0^{\Omega}(\Omega-\beta)^{k-\varphi-1}\frac{\partial^{k}\mathcal{W}(\Psi,\beta)}{\partial\Omega^{k}}\mathrm{d}\beta,\\ &\quad k-1<\varphi<k.\end{aligned} \tag{5}$$

$$\mathcal{D}_{\Omega}^{k}\mathcal{W}(\Psi,\Omega) = \frac{\partial^{k}\mathcal{W}(\Psi,\Omega)}{\partial\Omega^{k}},\quad k\in N.$$

Definition 2.4. If $\mathcal{W}(\Psi,\Omega)$ expresses the Caputo fractional derivate of the function $\mathcal{W}(\Psi,\Omega)$, then its Laplace transform is presented as follows [33–35]:

$$\begin{aligned}\mathcal{L}[\mathcal{D}_{\Omega}^{\varphi}\mathcal{W}(\Psi,\Omega)] &= s^{\varphi}-\sum_{p=0}^{k-1}s^{\varphi-p-1}\mathcal{W}^{(p)}(0^{+}),\\ &\quad (k-1<\varphi\le k),\end{aligned} \tag{6}$$

where $\mathcal{M}(s)$ represents the Laplace transform of the function $\mathcal{W}(\Psi,\Omega)$.

3 OAFM methodology

To widen the scope of the OAFM's effectiveness, it is essential that one consider its utilization inside the framework of partial differential equations. The basic partial differential equation (PDE) is typically represented as follows:

$$\mathbb{X}[\mathcal{W}(\Psi,\Omega)]+\Re(\Psi,\Omega)+\Upsilon[\mathcal{W}(\Psi,\Omega)]=0, \tag{7}$$

subjected to ICs,

$$\mathfrak{B}\left(\mathcal{W},\frac{\partial\mathcal{W}}{\partial\Omega}\right)=0, \tag{8}$$

where operators denoting linear and nonlinear functions are symbolized with the symbols $\mathbb{X}$ and Υ, respectively. $\Re$ denotes the source function, whereas the unknown function is denoted by $\mathcal{W}(\Psi,\Omega)$.

The task of finding the exact solutions of highly nonlinear equations is a considerable difficulty. The following equation presents the approximated solution.

$$\tilde{\mathcal{W}}(\Psi,\Omega)=\mathcal{W}_0(\Psi,\Omega)+\mathcal{W}_1(\Psi,\Omega,\Theta_{\mathbb{i}})\quad \mathbb{i}=1,2,\ldots\ \mathbb{j}. \tag{9}$$

To derive the first order approximation, Eq. (9) is substituted into Eq. (7), leading to the following expression:

$$\begin{aligned}&[\mathcal{W}_0(\Psi,\Omega)]+\mathbb{X}[\mathcal{W}_1((\Psi,\Omega),\Theta_{\mathbb{i}})]\\ &\quad=\Re(\Psi,\Omega)+\Upsilon[\mathcal{W}_0(\Psi,\Omega)+\mathcal{W}_1(\Psi,\Omega,\Theta_{\mathbb{i}})]=0.\end{aligned} \tag{10}$$

To obtain initial approximation, the following equation is utilized:

$$\mathbb{X}[\mathcal{W}_0(\Psi, \Omega) + \Re(\Psi, \Omega)] = 0, \quad \mathfrak{B}\left(\mathcal{W}_0, \frac{\partial \mathcal{W}_0}{\partial \Omega}\right) = 0. \tag{11}$$

Similarly, we can achieve $\mathcal{W}_1(\Psi, \Omega)$, *i.e.*, first-order approximation as follows:

$$\begin{aligned} &\mathbb{X}[\mathcal{W}_1(\Psi, \Omega, \Theta_{\mathbb{i}})] + \Upsilon[\mathcal{W}_0(\Psi, \Omega) + \mathcal{W}_1(\Psi, \Omega, \Theta_{\mathbb{i}})] = 0, \\ &\mathfrak{B}\left(\mathcal{W}_1, \frac{\partial \mathcal{W}_1}{\partial \Omega}\right) = 0. \end{aligned} \tag{12}$$

The following is the expression for the expansion of the nonlinear term.

$$\begin{aligned} &\Upsilon[\mathcal{W}_0(\Psi, \Omega) + \mathcal{W}_1(\Psi, \Omega, \Theta_{\mathbb{i}})] \\ &\quad = \Upsilon[\mathcal{W}_0(\Psi, \Omega)] + \sum_{b=1}^{\infty} \frac{\mathcal{W}_1^b}{b!} \Upsilon^{(b)}[\mathcal{W}_0(\Psi, \Omega)]. \end{aligned} \tag{13}$$

To effectively tackle the difficulties associated with solving Eq. (12) and enhance the rapid convergence of the first-order approximation $\mathcal{W}_1(\Psi, \Omega, \Theta_{\mathbb{i}})$ and the estimated solution $\tilde{\mathcal{W}}(\Psi, \Omega)$, we propose an alternative formulation to substitute the existing term in Eq. (12). This alteration enables the formulation of Eq. (12) in the following manner:

$$\left.\begin{aligned} &\mathbb{X}[\mathcal{W}_1(\Psi, \Omega, \Theta_{\mathbb{i}})] + \mathbb{U}_1[\mathcal{W}_0(\Psi, \Omega)]\Upsilon[\mathcal{W}_0(\Psi, \Omega)] \\ &\quad + \mathbb{U}_2[\mathcal{W}_0(\Psi, \Omega), \Theta_{\mathbb{j}}] = 0, \\ &\mathfrak{B}\left(\mathcal{W}_1, \frac{\partial \mathcal{W}_1}{\partial \Omega}\right) = 0. \end{aligned}\right\} \tag{14}$$

Remark I. The auxiliary functions $\mathbb{U}_1$ and $\mathbb{U}_2$, as illustrated in Eq. (14), rely upon the initial approximation $\mathcal{W}_0(\Psi, \Omega)$ and a set of unknown parameters $\Theta_{\mathbb{i}}$ and $\Theta_{\mathbb{j}}$, $\mathbb{i} = 1,2,3 \ldots \mathbb{s}$, $\mathbb{j} = \mathbb{s} + 1, \mathbb{s} + 2, \ldots . \mathbb{d}$.

Remark II. The auxiliary functions $\mathbb{U}_1$ and $\mathbb{U}_2$ exhibit an absence of uniqueness and have a similar form as $\mathcal{W}_0(\Psi, \Omega)$. This arrangement can be represented as $\Upsilon[\mathcal{W}_0(\Psi, \Omega)]$, or a combination of $\Upsilon[\mathcal{W}_0(\Psi, \Omega)]$ and $\mathcal{W}_0(\Psi, \Omega)$.

Remark III. The auxiliary functions will exhibit polynomial behavior if $\mathcal{W}_0(\Psi, \Omega)$ and $\Upsilon[\mathcal{W}_0(\Psi, \Omega)]$ are polynomial functions. Similarly, they will display exponential behavior if $\mathcal{W}_0(\Psi, \Omega)$ and $\Upsilon[\mathcal{W}_0(\Psi, \Omega)]$ are exponential functions. Likewise, if $\mathcal{W}_0(\Psi, \Omega)$ and $\Upsilon[\mathcal{W}_0(\Psi, \Omega)]$ are trigonometric functions, the auxiliary functions will manifest trigonometric behavior. If $\Upsilon[\mathcal{W}_0(\Psi, \Omega)] = 0$, then the initial guess will correspond to the exact solution of the original problem.

The convergence control parameters $\Theta_{\mathbb{i}}$ and $\Theta_{\mathbb{j}}$ are determined using the least square approach. In this particular context, we introduce the functional that integrates the convergence control parameters within the designated area.

$$\mathcal{M}(\Theta_{\mathbb{i}}, \Theta_{\mathbb{j}}) = \int_0^{\Omega}\int_0^{\Psi} \mathbb{E}^2(\Psi, \Omega, \Theta_{\mathbb{i}}, \Theta_{\mathbb{j}}) d\Psi d\Omega, \tag{15}$$

where $\mathbb{E}$ expresses the residual.

$$\begin{aligned} \mathbb{E}(\Psi, \Omega, \Theta_{\mathbb{i}}, \Theta_{\mathbb{j}}) &= \mathbb{X}[\tilde{\mathcal{W}}(\Psi, \Omega, \Theta_{\mathbb{i}}, \Theta_{\mathbb{j}})] + \Re(\Psi, \Omega) \\ &\quad + \Upsilon[\tilde{\mathcal{W}}(\Psi, \Omega, \Theta_{\mathbb{i}}, \Theta_{\mathbb{j}})], \\ \mathbb{i} &= 1, 2, 3 \ldots \mathbb{s}, \ \mathbb{j} = \mathbb{s} + 1, \mathbb{s} + 2, \ldots . \mathbb{d} \\ \frac{\partial \mathcal{M}_1}{\partial \Theta_1} &= \frac{\partial \mathcal{M}_2}{\partial \Theta_2} = \frac{\partial \mathcal{M}_3}{\partial \Theta_3} \ldots \ldots \ldots \frac{\partial \mathcal{M}_n}{\partial \Theta_n} = 0. \end{aligned} \tag{16}$$

The equation mentioned earlier is employed to determine the numerical values of the convergence control parameters.

4 Basic idea of LITM

To explain the fundamental concept of the iterative Laplace transform method, we examine a general space-time fractional partial differential equation accompanied by a starting condition in the following format:

$$\begin{aligned} \mathcal{D}_{\Omega}^{\varphi}\mathcal{W} = \mathcal{H}(\mathcal{W}, \mathcal{D}_{\Psi}^{\omega}\mathcal{W}, \mathcal{D}_{\Psi}^{2\omega}\mathcal{W}, \ldots .), \quad a - 1 < \varphi \le a, \\ b - 1 < \omega \le b, \quad a, b \in \mathcal{N}, \end{aligned} \tag{17}$$

subjected to ICs

$$\mathcal{W}^{(\varpi)}(\Psi, 0) = \mathcal{X}_{\varpi}(\Psi), \varpi = 0, 1, 2, 3 \ldots \ldots ., \quad a - 1. \tag{18}$$

Here, $\mathcal{H}(\mathcal{W}, \mathcal{D}_{\Psi}^{\omega}\mathcal{W}, \mathcal{D}_{\Psi}^{2\omega}\mathcal{W}, \ldots .)$ is a linear or nonlinear operator of $\mathcal{W}$, $\mathcal{D}_{\Psi}^{\omega}\mathcal{W}$, $\mathcal{D}_{\Psi}^{2\omega}\mathcal{W}$,....., and the unknown function $\mathcal{W} = \mathcal{W}(\Psi, \Omega)$ will be established later.

After taking Laplace transform of both sides of Eq. (17), we achieved

$$\begin{aligned} s^{\varphi}\mathcal{L}[\mathcal{W}(\Psi, \Omega)] - \sum_{\varpi=0}^{a-1} s^{\varphi-1-\varpi}\mathcal{W}^{(\varpi)}(\Psi, 0), \\ = \mathcal{L}[\mathcal{H}(\mathcal{W}, \mathcal{D}_{\Psi}^{\omega}\mathcal{W}, \mathcal{D}_{\Psi}^{2\omega}\mathcal{W}, \ldots .)]. \end{aligned} \tag{19}$$

In an equivalent manner,

$$\begin{aligned} \mathcal{L}[\mathcal{W}(\Psi, \Omega)] = \sum_{\varpi=0}^{a-1} s^{-1-\varpi}\mathcal{W}^{(\varpi)}(\Psi, 0) \\ + s^{-\varphi}\mathcal{L}[\mathcal{H}(\mathcal{W}, \mathcal{D}_{\Psi}^{\omega}\mathcal{W}, \mathcal{D}_{\Psi}^{2\omega}\mathcal{W}, \ldots .)], \end{aligned} \tag{20}$$

by applying the Laplace inverse operator to both sides of Eq. (20), we received

$$\begin{aligned} \mathcal{W}(\Psi, \Omega) = \mathcal{L}^{-1}\left[\sum_{\varpi=0}^{a-1} s^{-1-\varpi}\mathcal{W}^{(\varpi)}(\Psi, 0)\right] \\ + \mathcal{L}^{-1}[s^{-\varphi}\mathcal{L}[\mathcal{H}(\mathcal{W}, \mathcal{D}_{\Psi}^{\omega}\mathcal{W}, \mathcal{D}_{\Psi}^{2\omega}\mathcal{W}, \ldots .)]]. \end{aligned} \tag{21}$$

This can be expressed in a manner as follows:

$$\mathcal{W}(\Psi,\Omega) = \mathcal{L}^{-1}\left[\sum_{\varpi=0}^{a-1} s^{-1-\varpi}\mathcal{W}^{(\varpi)}(\Psi,0)\right] + \mathcal{F}(\mathcal{W}, \mathcal{D}_{\Psi}^{\omega}\mathcal{W}, \mathcal{D}_{\Psi}^{2\omega}\mathcal{W}, \ldots.), \tag{22}$$

here

$$\mathcal{F}(\mathcal{W}, \mathcal{D}_{\Psi}^{\omega}\mathcal{W}, \mathcal{D}_{\Psi}^{2\omega}\mathcal{W}, \ldots.) = \mathcal{L}^{-1}[s^{-\varphi}\mathcal{L}[\mathcal{H}(\mathcal{W}, \mathcal{D}_{\Psi}^{\omega}\mathcal{W}, \mathcal{D}_{\Psi}^{2\omega}\mathcal{W}, \ldots.)]].$$

The LITM is a mathematical technique that expresses the solution as an infinite series.

$$\mathcal{W}(\Psi,\Omega) = \sum_{c=0}^{\infty}\mathcal{W}_c, \tag{23}$$

where the term $\mathcal{W}_n$ can be computed iteratively. The operator $\mathcal{F}(\mathcal{W}, \mathcal{D}_{\Psi}^{\omega}\mathcal{W}, \mathcal{D}_{\Psi}^{2\omega}\mathcal{W}, \ldots.)$ can be divided into linear or nonlinear components as follows:

$$\begin{aligned}&\mathbb{B}\left(\sum_{c=0}^{\infty}\mathcal{W}_c, \mathcal{D}_{\Psi}^{\omega}\sum_{c=0}^{\infty}\mathcal{W}_c, \mathcal{D}_{\Psi}^{2\omega}\sum_{c=0}^{\infty}\mathcal{W}_c, \ldots\ldots\right)\\ &= \mathcal{F}(\mathcal{W}_0, \mathcal{D}_{\Psi}^{\omega}\mathcal{W}_0, \mathcal{D}_{\Psi}^{2\omega}\mathcal{W}_0, \ldots.)\\ &\quad + \sum_{c=1}^{\infty}\mathcal{F}\left(\sum_{\varpi=0}^{c}\mathcal{W}_{\varpi}, \mathcal{D}_{\Psi}^{\omega}\sum_{\varpi=0}^{c}\mathcal{W}_{\varpi}, \mathcal{D}_{\Psi}^{2\omega}\sum_{\varpi=0}^{c}\mathcal{W}_{\varpi}, \ldots\ldots\right)\\ &\quad - \sum_{c=1}^{\infty}\mathcal{F}\left(\sum_{\varpi=0}^{c-1}\mathcal{W}_{\varpi}, \mathcal{D}_{\Psi}^{\omega}\sum_{\varpi=0}^{c-1}\mathcal{W}_{\varpi}, \mathcal{D}_{\Psi}^{2\omega}\sum_{\varpi=0}^{c-1}\mathcal{W}_{\varpi}, \ldots\ldots\right).\end{aligned} \tag{24}$$

By substituting Eqs. (23) and (24) into Eq. (22), we achieved,

$$\begin{aligned}&\sum_{c=0}^{\infty}\mathcal{W}_c = \mathcal{L}^{-1}\left[\sum_{\varpi=0}^{a-1} s^{-1-\varpi}\mathcal{W}^{(\varpi)}(\Psi,0)\right]\\ &+ \mathcal{F}(\mathcal{W}_0, \mathcal{D}_{\Psi}^{\omega}\mathcal{W}_0, \mathcal{D}_{\Psi}^{2\omega}\mathcal{W}_0, \ldots.)\\ &+ \sum_{c=1}^{\infty}\mathcal{F}\left(\sum_{\varpi=0}^{c}\mathcal{W}_{\varpi}, \mathcal{D}_{\Psi}^{\omega}\sum_{\varpi=0}^{c}\mathcal{W}_{\varpi}, \mathcal{D}_{\Psi}^{2\omega}\sum_{\varpi=0}^{c}\mathcal{W}_{\varpi}, \ldots\ldots\right)\\ &- \sum_{c=1}^{\infty}\mathcal{F}\left(\sum_{\varpi=0}^{c-1}\mathcal{W}_{\varpi}, \mathcal{D}_{\Psi}^{\omega}\sum_{\varpi=0}^{c-1}\mathcal{W}_{\varpi}, \mathcal{D}_{\Psi}^{2\omega}\sum_{\varpi=0}^{c-1}\mathcal{W}_{\varpi}, \ldots\ldots\right).\end{aligned} \tag{25}$$

We format

$$\begin{aligned}&\mathcal{W}_0 = \mathcal{L}^{-1}\left[\sum_{\varpi=0}^{a-1} s^{-1-\varpi}\mathcal{W}^{(\varpi)}(\Psi,0)\right]\\ &\mathcal{W}_1 = \mathcal{F}(\mathcal{W}_0, \mathcal{D}_{\Psi}^{\omega}\mathcal{W}_0, \mathcal{D}_{\Psi}^{2\omega}\mathcal{W}_0, \ldots.)\\ &\mathcal{W}_{a+1} = \mathcal{F}\left(\sum_{\varpi=0}^{a}\mathcal{W}_{\varpi}, \mathcal{D}_{\Psi}^{\omega}\sum_{\varpi=0}^{a}\mathcal{W}_{\varpi}, \mathcal{D}_{\Psi}^{2\omega}\sum_{\varpi=0}^{a}\mathcal{W}_{\varpi}, \ldots\ldots\right),\\ &\mathcal{F}\left(\sum_{\varpi=0}^{a-1}\mathcal{W}_{\varpi}, \mathcal{D}_{\Psi}^{\omega}\sum_{\varpi=0}^{a-1}\mathcal{W}_{\varpi}, \mathcal{D}_{\Psi}^{2\omega}\sum_{\varpi=0}^{a-1}\mathcal{W}_{\varpi}, \ldots\ldots\right), a \geq 1.\end{aligned} \tag{26}$$

The last solution is obtained as follows:

$$\mathcal{W}(\Psi,\Omega) \cong \mathcal{W}_0(\Psi,\Omega) + \mathcal{W}_1(\Psi,\Omega) + \ldots + \mathcal{W}_a(\Psi,\Omega), \quad a = 1, 2, 3 \ldots. \tag{27}$$

5 Applications

5.1 Problem 1

5.1.1 Solution using OAFM

Let us consider Eq. (1), subjected to the initial condition [38] as follows:

$$\mathcal{W}(\Psi,0) = 3b\,\mathrm{sech}^2\left[\frac{1}{2}\sqrt{\frac{b}{1+b}}\Psi\right]. \tag{28}$$

Linear and nonlinear terms in Eq. (1) are as follows:

$$\mathbb{X}[\mathcal{W}(\Psi,\Omega)] = \frac{\partial^{\varphi}\mathcal{W}(\Psi,\Omega)}{\partial\Omega^{\varphi}}, \tag{29}$$

$$\Upsilon[\mathcal{W}(\Psi,\Omega)] = \frac{\partial\mathcal{W}}{\partial\Psi} + \mathcal{W}\frac{\partial\mathcal{W}}{\partial\Psi} + \frac{\partial^3\mathcal{W}}{\partial\Psi^2\partial\Omega}. \tag{30}$$

Exact solution of Eq. (1) when $\varphi = 1$ is given by [38]:

$$\mathcal{W}(\Psi,\Omega) = 3b\,\mathrm{sech}^2\left[\frac{1}{2}\sqrt{\frac{b}{1+b}}(\Psi - (1+b)\Omega)\right]. \tag{31}$$

The following equation illustrates the initial approximation:

$$\frac{\partial^{\varphi}\mathcal{W}_0(\Psi,\Omega)}{\partial\Omega^{\varphi}} = 0. \tag{32}$$

The result produced through the use of the inverse operator is as follows:

$$\mathcal{W}_0(\Psi,\Omega) = 3b\,\mathrm{sech}^2\left[\frac{1}{2}\sqrt{\frac{b}{1+b}}\Psi\right]. \tag{33}$$

By substituting Eq. (33) into Eq. (30), the resulting expression yields the nonlinear component as follows:

$$\begin{aligned}&\Upsilon[\mathcal{W}_0(\Psi,\Omega)]\\ &= -\frac{3}{2}b\sqrt{\left(\frac{b}{1+b}\right)}\left(1 + 6b + \cosh\left[\sqrt{\frac{b}{1+b}}\Psi\right]\right)\\ &\quad \times \mathrm{sech}\left[\frac{1}{2}\sqrt{\frac{b}{1+b}}\Psi\right]^4 \tanh\left[\frac{1}{2}\sqrt{\frac{b}{1+b}}\Psi\right].\end{aligned} \tag{34}$$

The selection of auxiliary functions is made as follows:

$$\mathbb{U}_1 = \Theta_1\left(3b\,\mathrm{sech}^2\left[\frac{1}{2}\sqrt{\frac{b}{1+b}}\,\Psi\right]\right)^2 + \Theta_2\left(3b\,\mathrm{sech}^2\left[\frac{1}{2}\sqrt{\frac{b}{1+b}}\,\Psi\right]\right)^4, \tag{35}$$

$$\mathbb{U}_2 = \Theta_3\left(3b\,\mathrm{sech}^2\left[\frac{1}{2}\sqrt{\frac{b}{1+b}}\,\Psi\right]\right)^6 + \Theta_4\left(3b\,\mathrm{sech}^2\left[\frac{1}{2}\sqrt{\frac{b}{1+b}}\,\Psi\right]\right)^8. \tag{36}$$

The standard statement of the first-order OAFM approximation is as follows:

$$\frac{\partial^{\varphi}\mathcal{W}_1(\Psi,\Omega,\Theta_i)}{\partial\Omega^{\varphi}} = -[\mathbb{U}_1[\mathcal{W}_0(\Psi,\Omega)]\Upsilon[\mathcal{W}_0(\Psi,\Omega)] + \mathbb{U}_2[\mathcal{W}_0(\Psi,\Omega),\Theta_j]]. \tag{37}$$

By finding Eq. (37) and then applying the inverse operator, we obtain the first-order approximation as follows:

$$\begin{aligned}\mathcal{W}_1(\Psi,\Omega) = {} & \frac{27\Omega^{\varphi}}{16\varphi\Gamma\varphi}b^3\,\mathrm{sech}\left[\frac{1}{2}\sqrt{\frac{b}{1+b}}\,\Psi\right]^{12}\Bigg[\Bigg(-432b^3\Theta_3 \\ & - 3{,}888b^5\Theta_4\,\mathrm{sech}\left[\frac{1}{2}\sqrt{\frac{b}{1+b}}\,\Psi\right]^4\Bigg) \\ & + \sqrt{\frac{b}{1+b}}\left(1+6b+\cosh\left[\sqrt{\frac{b}{1+b}}\,\Psi\right]\right) \\ & \times\Bigg(\Bigg(3\Theta_1+72b^2\Theta_2+4\Theta_1\cosh\left[\sqrt{\frac{b}{1+b}}\,\Psi\right] \\ & + \Theta_1\cosh\left[2\sqrt{\frac{b}{1+b}}\,\Psi\right]\Bigg)\tanh \\ & \times\left[\frac{1}{2}\sqrt{\frac{b}{1+b}}\,\Psi\right]\Bigg)\Bigg].\end{aligned} \tag{38}$$

According to OAFM,

$$\widetilde{\mathcal{W}}(\Psi,\Omega) = \mathcal{W}_0(\Psi,\Omega) + \mathcal{W}_1(\Psi,\Omega). \tag{39}$$

The convergence parameters for Eq. (39) are given as follows:

$$\Theta_1 = 562.511281098265;\ \Theta_2 = -79087.0489706844;$$
$$\Theta_3 = 310.7258673082475;\ \Theta_4 = -86285.58836719836.$$

5.1.2 Solution by LITM

Let us consider Eq. (1) with the initial condition as follows:

$$\mathcal{W}(\Psi,0) = 3b\,\mathrm{sech}^2\left[\frac{1}{2}\sqrt{\frac{b}{1+b}}\,\Psi\right]. \tag{40}$$

By applying Laplace transform to Eq. (1) using Eq. (40), we achieved,

$$\mathcal{L}[\mathcal{W}(\Psi,\Omega)] = \frac{3b\,\mathrm{sech}^2\left[\frac{1}{2}\sqrt{\frac{b}{1+b}}\,\Psi\right]}{s} + \frac{1}{s^{\varphi}}\mathcal{L}\left[-\frac{\partial\mathcal{W}}{\partial\Psi}\ \mathcal{W}\frac{\partial\mathcal{W}}{\partial\Psi} - \frac{\partial^3\mathcal{W}}{\partial\Psi^2\partial\Omega}\right]. \tag{41}$$

By applying inverse Laplace transform to Eq. (41), we achieved,

$$\mathcal{W}(\Psi,\Omega) = 3b\,\mathrm{sech}^2\left[\frac{1}{2}\sqrt{\frac{b}{1+b}}\,\Psi\right] + \mathcal{L}^{-1}\left[\frac{1}{s^{\varphi}}\mathcal{L}\left[-\frac{\partial\mathcal{W}}{\partial\Psi}\ \mathcal{W}\frac{\partial\mathcal{W}}{\partial\Psi} - \frac{\partial^3\mathcal{W}}{\partial\Psi^2\partial\Omega}\right]\right]. \tag{42}$$

By utilizing the LITM procedure, we obtained the approximation as follows:

$$\mathcal{W}_0(\Psi,\Omega) = 3b\,\mathrm{sech}^2\left[\frac{1}{2}\sqrt{\frac{b}{1+b}}\,\Psi\right], \tag{43}$$

$$\begin{aligned}\mathcal{W}_1(\Psi,\Omega) = {} & \frac{\Omega^{\varphi}3b\sqrt{\frac{b}{1+b}}}{2\Gamma(1+\varphi)}\Bigg[\Bigg(1+6b \\ & + \cosh\left[\sqrt{\frac{b}{1+b}}\,\Psi\right]\Bigg)\mathrm{sech}\left[\frac{1}{2}\sqrt{\frac{b}{1+b}}\,\Psi\right]^4 \\ & \tanh\left[\frac{1}{2}\sqrt{\frac{b}{1+b}}\,\Psi\right]\Bigg].\end{aligned} \tag{44}$$

In the same way, we can find $\mathcal{W}_2, \mathcal{W}_3 \ldots\ldots$

The last solution is achieved as follows:

$$\mathcal{W} = \mathcal{W}_0 + \mathcal{W}_1 + \ldots$$

5.2 Problem 2

5.2.1 Solution using OAFM

Let us consider the MRLW equation shown in Eq. (2), subjected to the initial condition [38] as follows:

$$\mathcal{W}(\Psi,0) = \sqrt{b}\,\mathrm{sech}\left[\left(\sqrt{\left(\frac{b}{\xi(1+b)}\right)}(\Psi-\lambda)\right)\right]. \tag{45}$$

Linear and nonlinear terms in Eq. (2) are as follows:

$$\mathbb{X}[\mathcal{W}(\Psi,\Omega)] = \frac{\partial^{\varphi}\mathcal{W}(\Psi,\Omega)}{\partial\Omega^{\varphi}}, \tag{46}$$

Table 1: Exact solution, OAFM solution, and LITM solution for distinct values of φ at $\Omega = 0.0001$ and $b = 0.02$ for problem 1

Ψ	Exact solution $\varphi = 1$	OAFM solution $\varphi = 1$	LITM solution $\varphi = 1$	OAFM solution $\varphi = 0.85$	LITM solution $\varphi = 0.85$
0.	0.059999999996	0.059999999999	0.060000000000	0.059999999998	0.060000000000
0.1	0.059997064916	0.059997065154	0.059997065154	0.059997085168	0.059997085168
0.2	0.059988248825	0.059988249299	0.059988249299	0.059988289319	0.059988289319
0.3	0.059973555181	0.059973555889	0.059973555889	0.059973615899	0.059973615899
0.4	0.059952989743	0.059952990685	0.059952990685	0.059953070660	0.059953070660
0.5	0.059926560567	0.059926561743	0.059926561743	0.059926661650	0.059926661650
0.6	0.059894278002	0.059894279410	0.059894279410	0.059894399209	0.059894399209
0.7	0.059856154678	0.059856156317	0.059856156317	0.059856295960	0.059856295960
0.8	0.059812205498	0.059812207367	0.059812207367	0.059812366795	0.059812366795
0.9	0.059762447624	0.059762449721	0.059762449721	0.059762628870	0.059762628871
1.	0.059706900465	0.059706902787	0.059706902788	0.059707101584	0.059707101586

$$\Upsilon[\mathcal{W}(\Psi,\Omega)] = \frac{\partial \mathcal{W}}{\partial \Psi} + 6\mathcal{W}^2\frac{\partial \mathcal{W}}{\partial \Psi} - \xi\frac{\partial^3 \mathcal{W}}{\partial \Psi^2 \partial \Omega}. \quad (47)$$

Exact solution of Eq. (2) when$\varphi = 1$ is given by the following equation [38]:

$$\mathcal{W}(\Psi,\Omega) = \sqrt{b}\,\operatorname{sech}\left[\left(\sqrt{\left(\frac{b}{\xi(1+b)}\right)}(\Psi - (b+1)\Omega - \lambda)\right)\right]. \quad (48)$$

The following equation presented illustrates the initial approximation.

$$\frac{\partial^{\varphi}\mathcal{W}_0(\Psi,\Omega)}{\partial \Omega^{\varphi}} = 0. \quad (49)$$

The result produced through the use of the inverse operator is as follows:

$$\mathcal{W}_0(\Psi,\Omega) = \sqrt{b}\,\operatorname{sech}\left[\left(\sqrt{\left(\frac{b}{\xi(1+b)}\right)}(\Psi - \lambda)\right)\right]. \quad (50)$$

By substituting Eq. (50) into Eq. (47), the resulting expression yields the nonlinear component as follows:

$$\begin{aligned}\Upsilon[\mathcal{W}_0(\Psi,\Omega)] = -\frac{1}{\sqrt{(1+b)\xi}}\Bigg[b\,\operatorname{sech}\left[\frac{\sqrt{b}(\Psi-\lambda)}{\sqrt{(1+b)\xi}}\right]\Bigg(1 \\ + 6b\,\operatorname{sech}\left[\frac{\sqrt{b}(\Psi-\lambda)}{\sqrt{(1+b)\xi}}\right]^2\Bigg)\tanh \\ \times\left[\frac{\sqrt{b}(\Psi-\lambda)}{\sqrt{(1+b)\xi}}\right]\Bigg].\end{aligned} \quad (51)$$

The selection of auxiliary functions is made as follows:

$$\begin{aligned}\mathbb{U}_1 = \Theta_1\left(\sqrt{b}\,\operatorname{sech}\left[\left(\sqrt{\left(\frac{b}{\xi(1+b)}\right)}(\Psi-\lambda)\right)\right]\right)^2 \\ + \Theta_2\left(\sqrt{b}\,\operatorname{sech}\left[\left(\sqrt{\left(\frac{b}{\xi(1+b)}\right)}(-\lambda)\right)\right]\right)^4,\end{aligned} \quad (52)$$

Table 2: Error analysis of problem 1 for distinct values of φ, at $\Omega = 0.0001$ and $b = 0.02$

Ψ	AE of OAFM $\varphi = 1$	AE of LITM $\varphi = 1$	AE of OAFM $\varphi = 0.85$	AE of LITM $\varphi = 0.85$
0.	$2.60394483 \times 10^{-12}$	$3.06000363 \times 10^{-12}$	$1.13997006 \times 10^{-12}$	$3.06000363 \times 10^{-12}$
0.1	$2.38189808 \times 10^{-10}$	$2.38320849 \times 10^{-10}$	$2.02520203 \times 10^{-8}$	$2.02525720 \times 10^{-8}$
0.2	$4.73384463 \times 10^{-10}$	$4.73384463 \times 10^{-10}$	$4.04937062 \times 10^{-8}$	$4.04937062 \times 10^{-8}$
0.3	$7.08075674 \times 10^{-10}$	$7.08055163 \times 10^{-10}$	$6.07181796 \times 10^{-8}$	$6.07180933 \times 10^{-8}$
0.4	$9.42137749 \times 10^{-10}$	$9.42137749 \times 10^{-10}$	$8.09173790 \times 10^{-8}$	$8.09173790 \times 10^{-8}$
0.5	$1.175424590 \times 10^{-9}$	$1.175437942 \times 10^{-9}$	$1.01083175 \times 10^{-7}$	$1.01083231 \times 10^{-7}$
0.6	$1.407762496 \times 10^{-9}$	$1.407762496 \times 10^{-9}$	$1.21207348 \times 10^{-7}$	$1.21207348 \times 10^{-7}$
0.7	$1.638943536 \times 10^{-9}$	$1.638919568 \times 10^{-9}$	$1.41281565 \times 10^{-7}$	$1.41281464 \times 10^{-7}$
0.8	$1.868719012 \times 10^{-9}$	$1.868719017 \times 10^{-9}$	$1.61297359 \times 10^{-7}$	$1.61297359 \times 10^{-7}$
0.9	$2.096793301 \times 10^{-9}$	$2.096972618 \times 10^{-9}$	$1.81246110 \times 10^{-7}$	$1.81246864 \times 10^{-7}$
1.	$2.322817979 \times 10^{-9}$	$2.323494346 \times 10^{-9}$	$2.01119022 \times 10^{-7}$	$2.01121869 \times 10^{-7}$

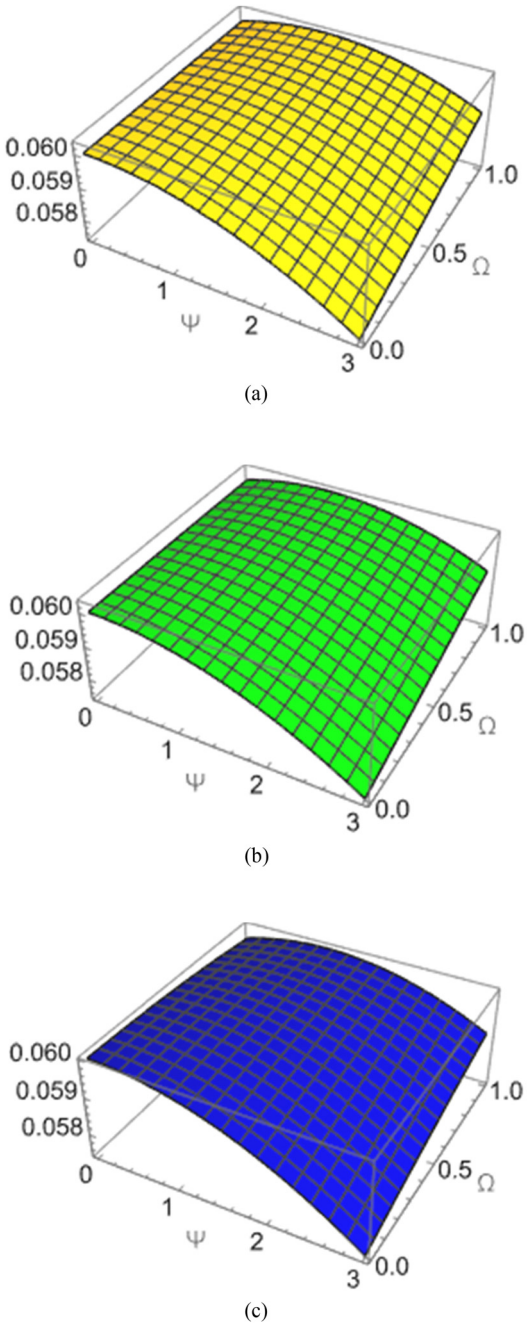

Figure 1: (a) The 3D visual of OAFM solution, (b) the 3D visual of LITM solution, and (c) the 3D visual of exact solution of the function $\mathscr{W}(\Psi, \Omega)$ at $\varphi = 1$ and $b = 0.02$ for problem 1.

$$\mathbb{U}_2 = \Theta_3\left(\sqrt{b}\,\operatorname{sech}\left[\left(\sqrt{\frac{b}{\xi(1+b)}}\right)(\Psi - \lambda)\right]\right)^6 + \Theta_4\left(\sqrt{b}\,\operatorname{sech}\left[\left(\sqrt{\frac{b}{\xi(1+b)}}\right)(-\lambda)\right]\right)^8. \quad (53)$$

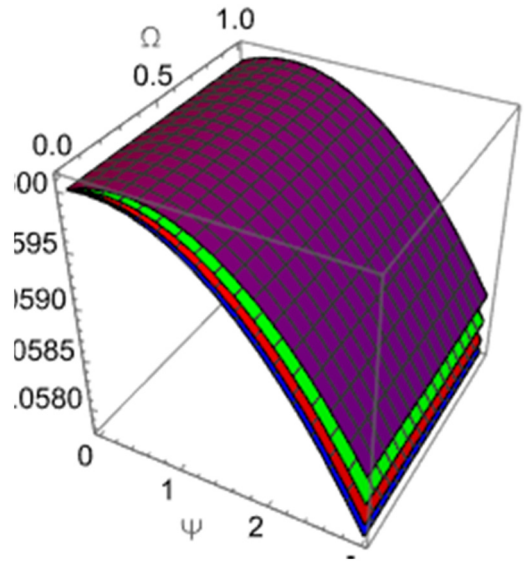

Figure 2: Comparison of 3D visuals at distinct values of φ using OAFM for problem 1.

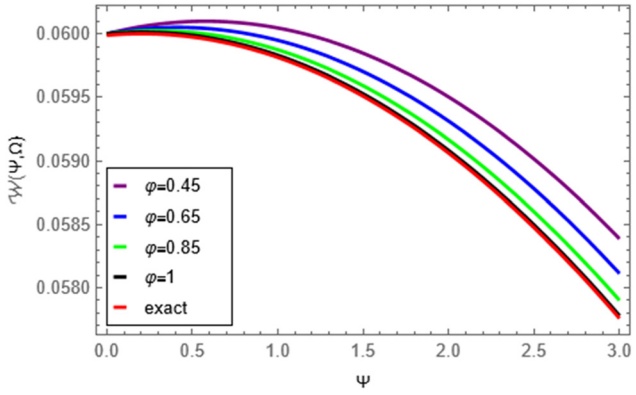

Figure 3: Comparison of 2D visuals at distinct values of φ for the function $\mathscr{W}(\Psi, \Omega)$ at $b = 0.02$.

The standard statement of the first-order OAFM approximation is as follows:

$$\frac{\partial^{\varphi}\mathcal{W}_1(\Psi, \Omega, \Theta_i)}{\partial\Omega^{\varphi}} = -[\mathbb{U}_1[\mathcal{W}_0(\Psi, \Omega)]\Upsilon[\mathcal{W}_0(\Psi, \Omega)] + \mathbb{U}_2[\mathcal{W}_0(\Psi, \Omega), \Theta_j]]. \quad (54)$$

Finding Eq. (54) and then applying the inverse operator, we obtain the first-order approximation as follows:

Table 3: Exact solution, OAFM solution, and LITM solution for distinct values of φ at $\Omega = 0.01$, $b = 0.001$, $\lambda = 10$, and $\xi = 1$ for problem (2)

Ψ	Exact solution $\varphi = 1$	OAFM solution $\varphi = 1$	LITM solution $\varphi = 1$	OAFM solution $\varphi = 0.85$	LITM solution $\varphi = 0.85$
0.	0.030103483941	0.030103472245	0.030103472244	0.030100223030	0.030100223029
0.1	0.030132499273	0.030132487661	0.030132487660	0.030129265767	0.030129265766
0.2	0.030161268989	0.030161257463	0.030161257463	0.030158063034	0.030158063034
0.3	0.030189791810	0.030189780371	0.030189780371	0.030186613551	0.030186613551
0.4	0.030218066464	0.030218055114	0.030218055114	0.030214916045	0.030214916045
0.5	0.030246091687	0.030246080428	0.030246080428	0.030242969250	0.030242969250
0.6	0.030273866225	0.030273855056	0.030273855056	0.030270771911	0.030270771911
0.7	0.030301388829	0.030301377754	0.030301377754	0.030298322780	0.030298322780
0.8	0.030328658262	0.030328647281	0.030328647281	0.030325620617	0.030325620617
0.9	0.030355673295	0.030355662408	0.030355662408	0.030352664192	0.030352664192
1.	0.030382432705	0.030382421915	0.030382421915	0.030379452284	0.030379452283

$$\begin{aligned}\mathcal{W}_1(\Psi,\Omega) = \frac{\Omega^{\varphi}}{\varphi\Gamma\varphi}\Bigg[\Bigg(&-b^3\Theta_3\operatorname{sech}\left[(\Psi-\lambda)\sqrt{\frac{b}{(1+b)\xi}}\right]^6\\ &- b^4\Theta_4\operatorname{sech}\left[(\Psi-\lambda)\sqrt{\frac{b}{(1+b)\xi}}\right]^8\Bigg)\\ &+ \frac{1}{\sqrt{(1+b)\xi}}\Bigg(b\Bigg(b\Theta_1\operatorname{sech}\left[(\Psi-\lambda)\sqrt{\frac{b}{(1+b)\xi}}\right]^2\\ &+ b^2\Theta_2\operatorname{sech}\left[(\Psi-\lambda)\sqrt{\frac{b}{(1+b)\xi}}\right]^4\Bigg)\\ &\times\Bigg(\operatorname{sech}\left[\frac{\sqrt{b}(\Psi-\lambda)}{\sqrt{(1+b)\xi}}\right]\\ &\times\left(1+6b\operatorname{sech}\left[\frac{\sqrt{b}(\Psi-\lambda)}{\sqrt{(1+b)\xi}}\right]^2\right)\tanh\left[\frac{\sqrt{b}(\Psi-\lambda)}{\sqrt{(1+b)\xi}}\right]\Bigg)\Bigg]\end{aligned}. \quad (55)$$

According to OAFM,

$$\tilde{\mathcal{W}}(\Psi,\Omega) = \mathcal{W}_0(\Psi,\Omega) + \mathcal{W}_1(\Psi,\Omega). \quad (56)$$

The convergence parameters for Eq. (56) are as follows:

$$\Theta_1 = 2582.258296906742; \Theta_2 = -1471956.734175127;$$

$$\Theta_3 = -460826.7010963857; \Theta_4 = 4.51492442310289 \times 10^8.$$

5.2.2 Solution by LITM

Let us consider the MRLW equation shown in Eq. (2), subjected to the initial condition [38] as follows:

$$\mathcal{W}(\Psi,0) = \sqrt{b}\operatorname{sech}\left[\left(\sqrt{\left(\frac{b}{\xi(1+b)}\right)}(\Psi-\lambda)\right)\right]. \quad (57)$$

By applying Laplace transform to Eq. (2) and using (57), we achieved

Table 4: Error analysis for problem 2 for distinct values of φ, at $\Omega = 0.01$, $b = 0.001$ $\lambda = 10$, and $\xi = 1$

Ψ	AE of OAFM $\varphi = 1$	AE of LITM $\varphi = 1$	AE of OAFM $\varphi = 0.85$	AE of LITM $\varphi = 0.85$
0.	$1.16965007 \times 10^{-8}$	$1.16970235 \times 10^{-8}$	$3.26091117 \times 10^{-6}$	$3.26091227 \times 10^{-6}$
0.1	$1.16118965 \times 10^{-8}$	$1.16120395 \times 10^{-8}$	$3.23350573 \times 10^{-6}$	$3.23350603 \times 10^{-6}$
0.2	$1.15257836 \times 10^{-8}$	$1.15257836 \times 10^{-8}$	$3.20595451 \times 10^{-6}$	$3.20595451 \times 10^{-6}$
0.3	$1.14382803 \times 10^{-8}$	$1.14382599 \times 10^{-8}$	$3.17825863 \times 10^{-6}$	$3.17825859 \times 10^{-6}$
0.4	$1.13494724 \times 10^{-8}$	$1.13494724 \times 10^{-8}$	$3.15041918 \times 10^{-6}$	$3.15041918 \times 10^{-6}$
0.5	$1.12594134 \times 10^{-8}$	$1.12594257 \times 10^{-8}$	$3.12243720 \times 10^{-6}$	$3.12243722 \times 10^{-6}$
0.6	$1.11681246 \times 10^{-8}$	$1.11681246 \times 10^{-8}$	$3.09431364 \times 10^{-6}$	$3.09431364 \times 10^{-6}$
0.7	$1.10755944 \times 10^{-8}$	$1.10755738 \times 10^{-8}$	$3.06604943 \times 10^{-6}$	$3.06604939 \times 10^{-6}$
0.8	$1.09817787 \times 10^{-8}$	$1.09817787 \times 10^{-8}$	$3.03764544 \times 10^{-6}$	$3.03764544 \times 10^{-6}$
0.9	$1.08866007 \times 10^{-8}$	$1.08867447 \times 10^{-8}$	$3.00910247 \times 10^{-6}$	$3.00910278 \times 10^{-6}$
1.	$1.07899506 \times 10^{-8}$	$1.07904773 \times 10^{-8}$	$2.98042128 \times 10^{-6}$	$2.98042240 \times 10^{-6}$

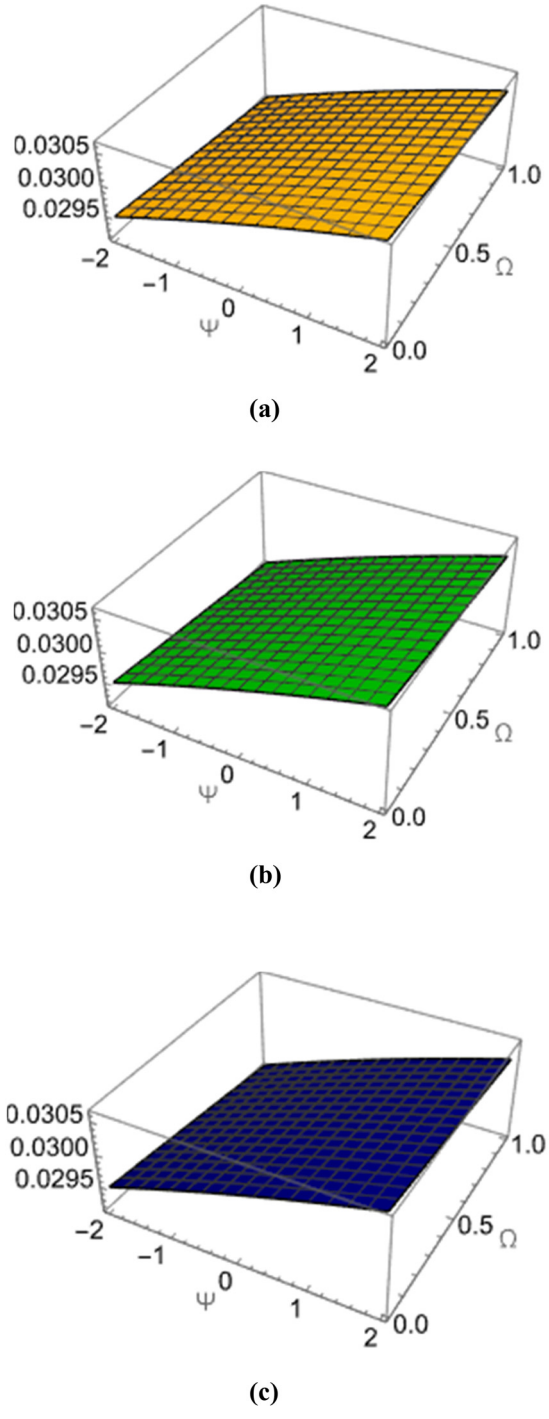

Figure 4: (a) The 3D visual of OAFM solution, (b) the 3D visual of LITM solution, (c) the 3D visual of exact solution of the function $\mathcal{W}(\Psi, \Omega)$ at $\varphi = 1$, $\Omega = 0.01$, $b = 0.001$, $\lambda = 10$, and $\xi = 1$ for problem 2.

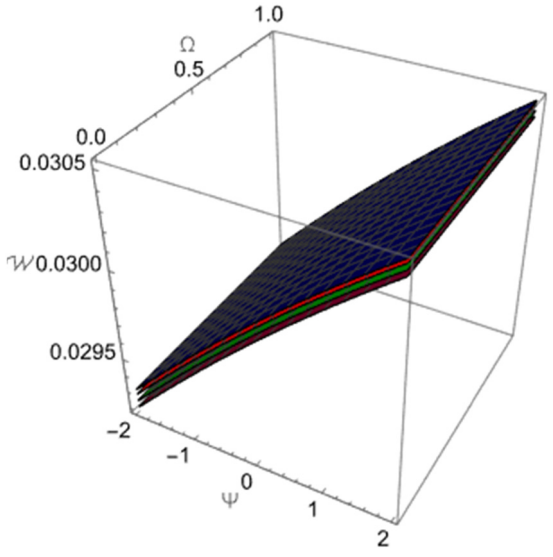

Figure 5: Comparison of 3D visuals at distinct values of φ using OAFM for problem 2.

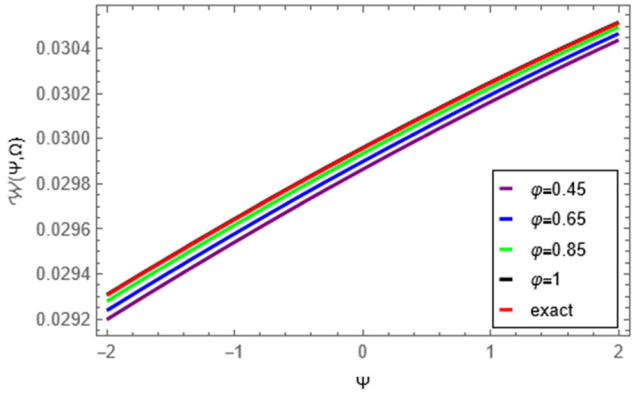

Figure 6: Comparison of 2D visuals at distinct values of φ for the function $\mathcal{W}(\Psi, \Omega)$ at $b = 0.001$, $\lambda = 10$, and $\xi = 1$ for problem (2).

$$\mathcal{L}[\mathcal{W}(\Psi, \Omega)] = \frac{\sqrt{b}\ \operatorname{sech}\left[\left(\sqrt{\left(\frac{b}{\xi(1+b)}\right)}(\Psi - \lambda)\right)\right]}{s} + \frac{1}{s^{\varphi}}\mathcal{L}\left[-\frac{\partial \mathcal{W}}{\partial \Psi} - 6\mathcal{W}^2\frac{\partial \mathcal{W}}{\partial \Psi} + \xi\frac{\partial^3 \mathcal{W}}{\partial \Psi^2 \partial \Omega}\right]. \tag{58}$$

By applying inverse Laplace transform to Eq. (58), we achieved

$$\mathcal{W}(\Psi, \Omega) = \sqrt{b}\ \operatorname{sech}\left[\left(\sqrt{\left(\frac{b}{\xi(1+b)}\right)}(\Psi - \lambda)\right)\right] + \mathcal{L}^{-1}\left[\frac{1}{s^{\varphi}}\mathcal{L}\left[-\frac{\partial \mathcal{W}}{\partial \Psi} - 6\mathcal{W}^2\frac{\partial \mathcal{W}}{\partial \Psi} + \xi\frac{\partial^3 \mathcal{W}}{\partial \Psi^2 \partial \Omega}\right]\right]. \quad (59)$$

By utilizing the LITM procedure, we obtained the approximation as follows:

$$\mathcal{W}_0(\Psi, \Omega) = \sqrt{b}\ \operatorname{sech}\left[\left(\sqrt{\left(\frac{b}{\xi(1+b)}\right)}(\Psi - \lambda)\right)\right],$$

$$\mathcal{W}_1(\Psi, \Omega) = \frac{\Omega^{\varphi}}{\sqrt{(1+b)\xi}\,\Gamma(1+\varphi)}\left[b\ \operatorname{sech}\left[\frac{\sqrt{b}(\Psi - \lambda)}{\sqrt{(1+b)\xi}}\right]\left(1 + 6b\ \operatorname{sech}\left[\frac{\sqrt{b}(\Psi - \lambda)}{\sqrt{(1+b)\xi}}\right]^2\right)\tanh\left[\frac{\sqrt{b}(\Psi - \lambda)}{\sqrt{(1+b)\xi}}\right]\right].$$

In the same way, we can find $\mathcal{W}_2, \mathcal{W}_3$ ……

The last solution achieved as $\mathcal{W} = \mathcal{W}_0 + \mathcal{W}_1 + \ldots$

6 Results and analysis

Table 1 in problem 1 exhibits the exact solution of Eq. (31), OAFM solution, and LITM solution of Eq. (1) at $\varphi = 1$, $\varphi = 0.85$ when $b = 0.02$ and $\Omega = 0.0001$, and Table 2 in problem 1 exhibits the absolute errors of OAFM solution and LITM solution of Eq. (1) at $\varphi = 1$, $\varphi = 0.85$ when $b = 0.02$ and $\Omega = 0.0001$. Figure 1(a) shows the 3D visuals of OAFM solution of Eq. (1) at $\varphi = 1$, $b = 0.02$, and $\Omega = 0.0001$. Figure 1(b) shows the 3D visuals of LITM solution of Eq. (1) at $\varphi = 1$, $b = 0.02$, and $\Omega = 0.0001$. Figure 1(c) represents the 3D visuals of exact solution of Eq. (31) at $b = 0.02$. Figure 2 in problem 1 highlights the comparison of 3D visuals of OAFM solution of Eq. (1) at distinct values of φ at $b = 0.02$. Figure 3 in problem 1 highlights the comparison of 2D visuals of OAFM solution of Eq. (1) and exact solution presented in Eq. (31) at distinct values of φ at $b = 0.02$. Table 3 in problem 2 exhibits the exact solution of Eq. (48), OAFM solution and LITM solution of Eq. (2) at $\varphi = 1$, $\varphi = 0.85$ when $\Omega = 0.01$, $b = 0.001$, $\lambda = 10$, and $\xi = 1$. Table 4 in problem 2 exhibits the absolute errors of OAFM solution and LITM solution of Eq. (2) at $\varphi = 1$, $\varphi = 0.85$ when $\Omega = 0.01$, $b = 0.001$, $\lambda = 10$, and $\xi = 1$. Figure 4(a) represents the 3D visuals of OAFM solution of Eq. (2) at $\varphi = 1$, when $\Omega = 0.01$, $b = 0.001$, $\lambda = 10$, and$\xi = 1$. Figure 4(b) represents the 3D visuals of LITM solution of Eq. (2) at φ =1, when $\Omega = 0.01$, $b = 0.001$,$\lambda = 10$, and $\xi = 1$. Figure 4(c) represents the 3D visuals of exact solution of Eq. (48) at $b = 0.001$, $\lambda = 10$, and $\xi = 1$. Figure 5 in problem 2 highlights the comparison of 3D visuals of OAFM solution of Eq. (2) at distinct values of φ when b = 0.001, $\lambda = 10$, and $\xi = 1$. Figure 6 in problem 2 highlights the comparison of 2D visuals of OAFM solution of Eq. (2) and exact solution presented in Eq. (48) at distinct values of φ when $b = 0.001$, $\lambda = 10$, and $\xi = 1$. This research study was done for solving the time-fractional nonlinear GRLW equation and time-fractional nonlinear MRLW equation using two computational methods, namely, the OAFM and LITM. The outcomes obtained from both techniques are nearly equal and strongly satisfy each other results.

7 Conclusion

This study examines the use of the OAFM and LITM approaches to solve time fractional RLW, nonlinear time-fractional GRLW, and time-fractional MRLW equations. The mathematical simulation program Mathematica 13.3 is employed for this purpose. The findings that were achieved play an essential part in the exploration of nonlinear physical systems that arise in both the pure and applied fields of science and engineering. This study demonstrates that the proposed methodologies are straightforward to execute, effective, and adaptable for a wide range of nonlinear equations. Both of these strategies are effective in reducing the size of mathematical calculations. The tables and figures demonstrate that as the parameter φ approaches the classical value of 1 in the given problem, the approximate solution converges to the precise solution.

Acknowledgments: The authors extend their appreciation to the Deanship of Scientific Research at King Khalid University for funding this work through the Small Group Research Project under grant number RGP1/216/44. This work was supported by the Deanship of Scientific Research, the Vice Presidency for Graduate Studies and Scientific Research, King Faisal University, Saudi Arabia (GrantA186).

Funding information: The authors extend their appreciation to the Deanship of Scientific Research at King Khalid University for funding this work through the Small Group Research Project under grant number RGP1/216/44. This work was supported by the Deanship of Scientific Research, the Vice Presidency for Graduate Studies and Scientific Research, King Faisal University, Saudi Arabia (GrantA186).

Author contributions: All authors have accepted responsibility for the entire content of this manuscript and approved its submission.

Conflict of interest: The authors state no conflict of interest.

References

[1] Lotfy Kh, El-Bary AA, Tantawi RS. Effects of variable thermal conductivity of a small semiconductor cavity through the fractional order heat-magneto-photothermal theory. Eur Phys J Plus. 2019;134(6):280.

[2] Kilbas AA, Srivastava HM, Trujillo JJ. Theory and applications of fractional differential equations. North-Holland mathematics studies. Vol. 204. Amsterdam, The Netherlands: Elsevier; 2006.

[3] Yasmin H, Alderremy AA, Shah R, Hamid Ganie A, Aly S. Iterative solution of the fractional Wu-Zhang equation under Caputo derivative operator. Front Phys. 2024;12:1333990.

[4] Alshammari S, Moaddy K, Alshammari M, Alsheekhhussain Z, Al-Sawalha MM, Yar M. Analysis of solitary wave solutions in the fractional-order Kundu–Eckhaus system. Sci Rep. 2024;14(1):3688.

[5] Cai X, Tang R, Zhou H, Li Q, Ma S, Wang D, et al. Dynamically controlling terahertz wavefronts with cascaded metasurfaces. Adv Photonics. 2021;3(3):036003. doi: 10.1117/1.AP.3.3.036003.

[6] Zhu C, Al-Dossari M, Rezapour S, Shateyi S. On the exact soliton solutions and different wave structures to the modified Schrödinger's equation. Results Phys. 2023;54:107037. doi: 10.1016/j.rinp.2023.107037.

[7] Zhu C, Al-Dossari M, El-Gawaad NSA, Alsallami SAM, Shateyi S. Uncovering diverse soliton solutions in the modified Schrödinger's equation via innovative approaches. Results Phys. 2023;54:107100. doi: 10.1016/j.rinp.2023.107100.

[8] Zhu C, Abdallah SAO, Rezapour S, Shateyi S. On new diverse variety analytical optical soliton solutions to the perturbed nonlinear Schrödinger equation. Results Phys. 2023;54:107046. doi: 10.1016/j.rinp.2023.107046.

[9] Zhu C, Idris SA, Abdalla MEM, Rezapour S, Shateyi S, Gunay B. Analytical study of nonlinear models using a modified Schrödinger's equation and logarithmic transformation. Results Phys. 2023;55:107183. doi: 10.1016/j.rinp.2023.107183.

[10] Kai Y, Yin Z. On the Gaussian traveling wave solution to a special kind of Schrödinger equation with logarithmic nonlinearity. Mod Phys Lett B. 2021;36(2):2150543. doi: 10.1142/S0217984921505436.

[11] Kai Y, Ji J, Yin Z. Study of the generalization of regularized long-wave equation. Nonlinear Dyn. 2022;107(3):2745–52. doi: 10.1007/s11071-021-07115-6.

[12] Gao N, Liu J, Deng J, Chen D, Huang Q, Pan G. Design and performance of ultra-broadband composite meta-absorber in the 200Hz-20kHz range. J Sound Vib. 2024;574:118229. doi: 10.1016/j.jsv.2023.118229.

[13] El-Tantawy SA, Matoog RT, Shah R, Alrowaily AW, Ismaeel SM. On the shock wave approximation to fractional generalized Burger–Fisher equations using the residual power series transform method. Phys Fluids. 2024;36(2):023105.

[14] Alsheekhhussain Z, Moaddy K, Shah R, Alshammari S, Alshammari M, Al-Sawalha MM, et al. Extension of the optimal auxiliary function method to solve the system of a fractional-order Whitham–Broer–Kaup equation. Fractal Fract. 2023;8(1):1.

[15] Amin M, Abbas M, Iqbal MK, Baleanu D. Numerical treatment of time-fractional Klein–Gordon equation using redefined extended cubic B-spline functions. Front Phys. 2020;8:288.

[16] Al-Sawalha MM, Mukhtar S, Shah R, Ganie AH, Moaddy K. Solitary waves propagation analysis in nonlinear dynamical system of fractional coupled Boussinesq-Whitham-Broer-Kaup equation. Fractal Fract. 2023;7:889.

[17] Kumar D, Singh J, Kumar S. Numerical computation of fractional multi-dimensional diffusion equations by using a modified homotopy perturbation method. J Assoc Arab Univ Basic Appl Sci. 2015;17:20–6.

[18] Alqhtani M, Saad KM, Shah R, Hamanah WM. Discovering novel soliton solutions for (3 + 1)-modified fractional Zakharov–Kuznetsov equation in electrical engineering through an analytical approach. Opt Quantum Electron. 2023;55(13):1149.

[19] Ganie AH, Yasmin H, Alderremy AA, Aly S. An efficient semi-analytical techniques for the fractional-order system of Drinfeld-Sokolov-Wilson equation. Phys Scr. 2024;99(1):015253.

[20] Khalifa AK, Raslan KR, Alzubaidi H. Numerical study using ADM for the modified regularized long wave equation. Appl Math Model. 2008;32(12):2962–72.

[21] Khan Y, Taghipour R, Falahian M, Nikkar A. A new approach to modified regularized long wave equation. Neural Comput Appl. 2013;23:1335–41.

[22] Bota C, Căruntu B. Approximate analytical solutions of the regularized long wave equation using the optimal homotopy perturbation method. Sci World J. 2014;2014:6.

[23] Achouri T, Omrani K. Numerical solutions for the damped generalized regularized long-wave equation with a variable coefficient by Adomian decomposition method. Commun Nonlinear Sci Numer Simul. 2009;14(5):2025–33.

[24] Olubanwo OO, Odetunde OS. Laplace homotopy perturbation method of solving nonlinear partial differential equations. Ann Computer Sci Ser. 2019;17(2):2.

[25] Benjamin TB, Bona JL, Mahony JJ. Model equations for long waves in nonlinear dispersive systems. Philos Trans R Soc Lond Ser A, Math Phys Sci. 1972;272(1220):47–78.

[26] Hammad MMA, Shah R, Alotaibi BM, Alotiby M, Tiofack CGL, Alrowaily AW, et al. On the modified versions of G′ G-expansion technique for analyzing the fractional coupled Higgs system. AIP Adv. 2023;13(10):105131.

[27] Marinca V, Herisanu N. An application of the optimal auxiliary functions to Blasius problem. Rom J Tech Sci Appl Mech. 2015;60(3):206–15.

[28] Marinca V, Marinca B. Optimal auxiliary functions method for nonlinear thin film flow of a third grade fluid on a moving belt. A A. 2018;2(2):1–2.

[29] Jafari H, Nazari M, Baleanu D, Khalique CM. A new approach for solving a system of fractional partial differential equations. Computers Math Appl. 2013;66(5):838–43.

[30] Noor S, Albalawi W, Shah R, Shafee A, Ismaeel SM, El-Tantawy SA. A comparative analytical investigation for some linear and nonlinear time-fractional partial differential equations in the framework of the Aboodh transformation. Front Phys. 2024;12:1374049.

[31] El-Ajou A, Arqub OA, Zhour ZA, Momani S. New results on fractional power series: theories and applications. Entropy. 2013;15(12):5305–23.

[32] El-Ajou A, Arqub OA, Momani S. Approximate analytical solution of the nonlinear fractional KdV–Burgers equation: A new iterative algorithm. J Comput Phys. 2015;293:81–95.
[33] Noor S, Albalawi W, Al-Sawalha MM, Ismaeel SM, El-Tantawy SA. On the approximations to fractional nonlinear damped Burger's-type equations that arise in fluids and plasmas using Aboodh residual power series and Aboodh transform iteration methods. Front Phys. 2024;12:1374481.
[34] Noor S, Albalawi W, Al-Sawalha MM, Ismaeel SM. Mathematical frameworks for investigating fractional nonlinear coupled Korteweg-de Vries and Burger's equations. Front Phys. 2024;12:1374452.
[35] Goswami A, Singh J, Kumar D, Gupta S. An efficient analytical technique for fractional partial differential equations occurring in ion acoustic waves in plasma. J Ocean Eng Sci. 2019;4(2):85–99.